Current Urology Reports (2019) 20: 5
https://doi.org/10.1007/s11934-019-0867-7

KIDNEY DISEASES (G CIANCIO, SECTION EDITOR)

Imaging of Unusual Renal Tumors

R. Patricia Castillo[1] · Juan Francisco Santoscoy[1] · Leonardo Pisani[1] · Beatrice L. Madrazo[1] · V. Javier Casillas[1]

Published online: 21 January 2019

Abstract
Purpose of Review Renal masses are a wide entity and a common finding in clinical practice. Detection of these masses has increased in the last years, yet mortality rates have slightly decreased.
Recent Findings According to the World Health Organization classification, there are 8 types, 51 subtypes, and a lot more subsequent subclassifications of renal tumors. Histopathological analysis should always be assessed for final diagnosis of theses tumors. However, imaging can be an important diagnostic guidance. The most common diagnoses of renal tumor are clear cell carcinoma, papillary renal cell carcinoma, angiomyolipoma, and transitional cell carcinoma. Nonetheless, a considerable variety of particular tumors can arise from the kidney, challenging the expertise of radiologists and urologists on this subject.
Summary The awareness of these unusual entities is vital for professionals working at a complex medical facility with greater volume of patients. We hereby present uncommon renal tumors and its pathological and radiological features.

Keywords Renal neoplasm · Renal cell tumor · Mesenchymal renal tumor · Mixed epithelial and stromal tumors · Imaging features

Introduction

Renal masses are a wide heterogeneous entity that is frequently diagnosed incidentally. The detection of small renal masses has increased due to the broad use of imaging studies and current higher life expectancies, becoming a very common finding in clinical practice. It is estimated that 65,000 new kidney cancers will be diagnosed in 2018 in the USA and 300,000 worldwide [1]. Notwithstanding the rising diagnosis rate, mortality rates from renal cell carcinoma (RCC) have slightly decreased in the last years [2].

The current classification of renal tumors (2016 World Health Organization classification) list 8 types of tumor and 51 subtypes based on cytoplasmatic, architectural, anatomic location, correlation with renal disease background and molecular features. Prognosis is determined fundamentally by pathological stage and is favorable (80–90% at 5 years) for most patients with localized disease (stage I–II). The Fuhrman grading system of renal tumors is recommended by the World Health Organization (WHO) and is the most frequently used grading system in RCC but has not been validated for most of the new subtypes of renal carcinoma [3].

The most common diagnoses of renal tumor are clear cell carcinoma, papillary renal cell carcinoma, angiomyolipoma, and transitional cell carcinoma. Nonetheless, a considerable variety of particular tumors can arise from the kidney, challenging the expertise of radiologists and urologists on this subject. The awareness of these unusual entities is vital for professionals working at a complex medical facility with greater volume of patients. We hereby present the pathological and radiological features of uncommon renal tumors.

This article is part of the Topical Collection on *Kidney Diseases*

✉ Juan Francisco Santoscoy
f.santoscoygtz@gmail.com

[1] Department of Radiology, University of Miami/Miller School of Medicine, 1611 NW 12th Avenue, Miami, FL 33136, USA

Renal Cell Tumors

Collecting Duct Carcinoma

Collecting duct carcinoma (CDC) is an uncommon subtype of RCC which account for less than 1% of all epithelial renal malignancies [4]. Males are more frequently affected showing a male-to-female ratio of approximately 2:1 and a mean age of 55 years [5, 6]. Hematuria and back pain is the most common clinical presentation [7].

Histologically, CDC is characterized by angulated tubules and glands with tubulopapillary growth pattern, presence of desmoplastic stroma with predominant lymphocytic inflammatory infiltrate, and intraluminal mucin production [6]. Immunohistochemically, it is reactive for vimentin and *Ulex europaeus* agglutinin 1 (UEA-1), variably for high molecular weight cytokeratin (HMW-CK), CK7 and Pax2, and negative for CD10 and α-methylacyl-CoA racemase (AMACR). Immunoreactivity for UEA1 is a hallmark of collecting duct carcinoma [4, 6].

Grossly, CDC typically appears as a gray-white deep medullary infiltrative neoplasm and a medullary epicenter may be seen on imaging. On ultrasound, CDC may be seen homogenously hyperechoic, isoechoic, or hypoechoic to renal parenchyma [8, 9]. On computed tomography (CT), it appear as a hypoattenuating and hypovascular solid mass (Fig. 1). T1-weighted imaging exhibits variable signal and low-signal intensity on T2-weighted images. On MR imaging, cystic changes with mural nodules can be seen [8]. On both CT and MR imaging, CDC demonstrates heterogeneous necrotic, hemorrhagic, and calcified areas. Calcification can be seen in up to 25% of cases [8, 9].

Although most cases of RCC can be successfully treated by surgical resection, postoperative recurrence and metastatic disease is not uncommon. CDC is an aggressive neoplasm with poor prognosis, and one-third of patients have metastatic disease at presentation, and about two-thirds of patients die within 2 years after diagnosis [5, 9].

Renal Medullary Cell Carcinoma

Renal medullary carcinoma (RMC) is a very rare RCC that accounts for 0.5% of all renal carcinomas and arise in the renal medulla from the renal papillae or calyceal epithelium [10]. Most frequently affects males and adolescent and young adult population between the first and third decade of live. They commonly presents as an abdominal mass with flank pain and painless hematuria and less frequently with weight loss and fever [10, 11].

This renal tumor is highly associated with sickle cell hemoglobinopathies, especially with sickle cell trait. It is believed that the chronic hypoxic environment of the renal medulla due to red blood cells sickling induce the strong expression of vascular endothelial growth factor and hypoxia-inducible factor [12].

Histologically, RMC is a poorly differentiated high-grade renal epithelial neoplasm that presents a reticular microcystic growth pattern and cribriform adenoid cystic component with a neutrophilic infiltrate associated with a desmoplastic and stromal inflammation [11, 13]. Presence of sickled RBCs in the specimen is pathognomonic and on immunohistochemical analysis, loss of SMARCB1/INI1 expression is diagnostic of RMC [10].

The right kidney is more commonly affected by RMC and appears as an infiltrative mass extending from the renal pelvicalyceal system [12]. On CT imaging, it is seen as an ill-defined heterogenous hypoenhancing renal mass in relation with the cortex and medulla (Fig. 2) [10, 13]. The tumor extension and invasion are better visualized on magnetic resonance imaging (MRI) and may be seen hypointense on T2-weighted images due to hemorrhagic foci with extensive necrotic areas [9, 13]. Caliectasis without pelviectasis is a common characteristic finding as well as perinephric fat extension and involvement of local lymph nodes. Metastatic disease is usually present at the time of diagnosis, commonly affecting lymph nodes, liver, and lung [14••]. Pulmonary metastases can be secondary to lymphangitic spread resulting in nodular thickening of the interlobular septa and interstitial thickening, which is specific for lymphangitic carcinomatosis. Hilar and/or mediastinal lymphadenopathy is associated in 50% of the cases [12].

RMC is a very aggressive tumor with poor prognosis and most cases are diagnosed in late stages. The mainstay of treatment is nephrectomy for localized disease and nephrectomy with retroperitoneal lymph node resection and platinum-based chemotherapy for metastatic disease [10, 11].

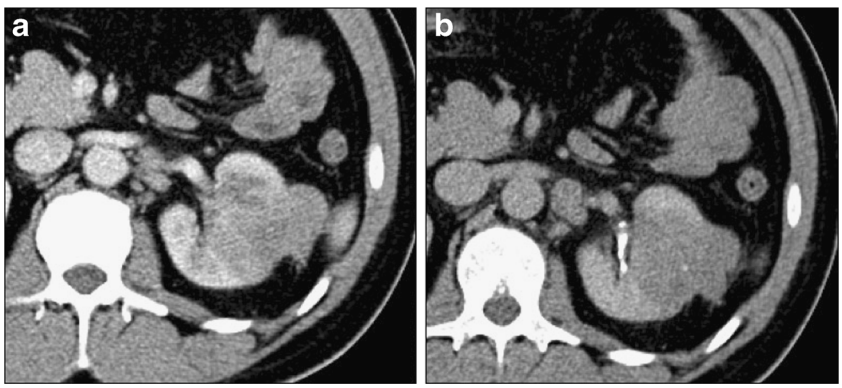

Fig. 1 Collecting duct carcinoma in a 44-year-old male with painless hematuria. Contrast-enhanced CT nephrographic (**a**) and delayed (**b**) phases images reveal a solid mass with a punctate calcification extending into the renal sinus and invading the perirenal fat

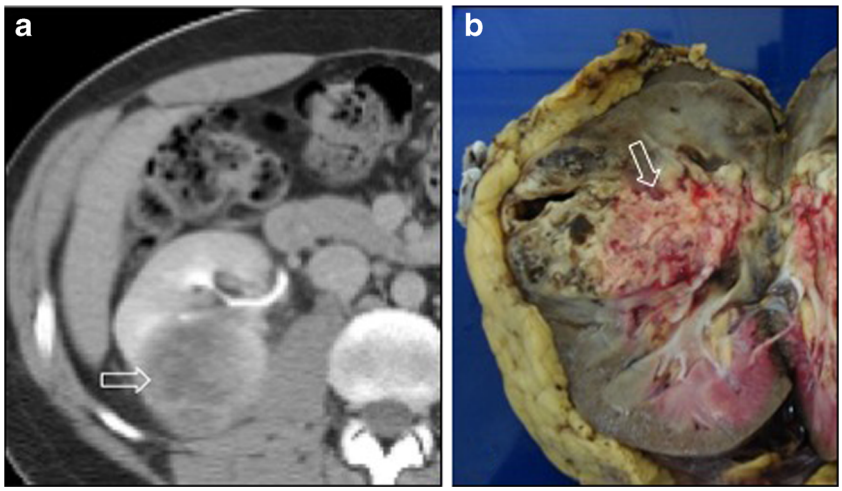

Fig. 2 Medullary renal cell carcinoma in a 22-year-old male with sickle cell trait, fever, and right flank pain. Contrast enhanced-CT axial (**a**) images reveal a large solid mass with central necrosis (arrow) in the interpolar region of the right kidney. Photograph of the sectioned mass (**b**) shows a necrotic mass in the right kidney (arrow)

Multilocular Cystic Renal Cell Carcinoma

Multilocular cystic renal cell carcinoma (MCRCC) was previously considered a subtype of clear cell RCC [15]. However, after the 2012 ISUP (International Society of Urological Pathology) Vancouver modification of the WHO classification, it has been re-designated as multilocular cystic renal neoplasm of low malignant potential given its low risk for metastasis and tumor recurrence. MCRCC is a very rare tumor, accounts to 1.5–4% of all RCCs and to 1–2% of all renal tumors, males are more commonly affected, and have a presentation mean age of 51 years [16, 17].

MCRCC is by definition a completely cystic tumor with absent solid mass-forming component [18]. Histologically, MCRCC demonstrate multiple septated gelatinous or hemorrhagic cysts lined by flattened cuboidal cells with clear cytoplasm. Calcifications can be found in the septa in more than 20% of the cases [19, 20]. Chromosome 3p deletion and von Hippel-Lindau (VHL) gene mutation has been shown in 74% and 25% of the cases of MCRCC, respectively [17].

MCRCC is commonly a unilateral solitary well-defined mass. On CT imaging, multiple cysts with regular septations with moderate contrast-enhancement are seen (Fig. 3) [8]. On MR imaging, the cyst fluid signal intensity may vary depending on the content, however, commonly are hyperintense due to the proteinaceous or hemorrhagic composition on T1- and T2-weighted images. The capsule shows low-signal intensity on T1- and T2-weighted imaging due to its fibrous component [8, 19]. It is important to mention that for tumors smaller than 30 mm, imaging features are not reliable to completely

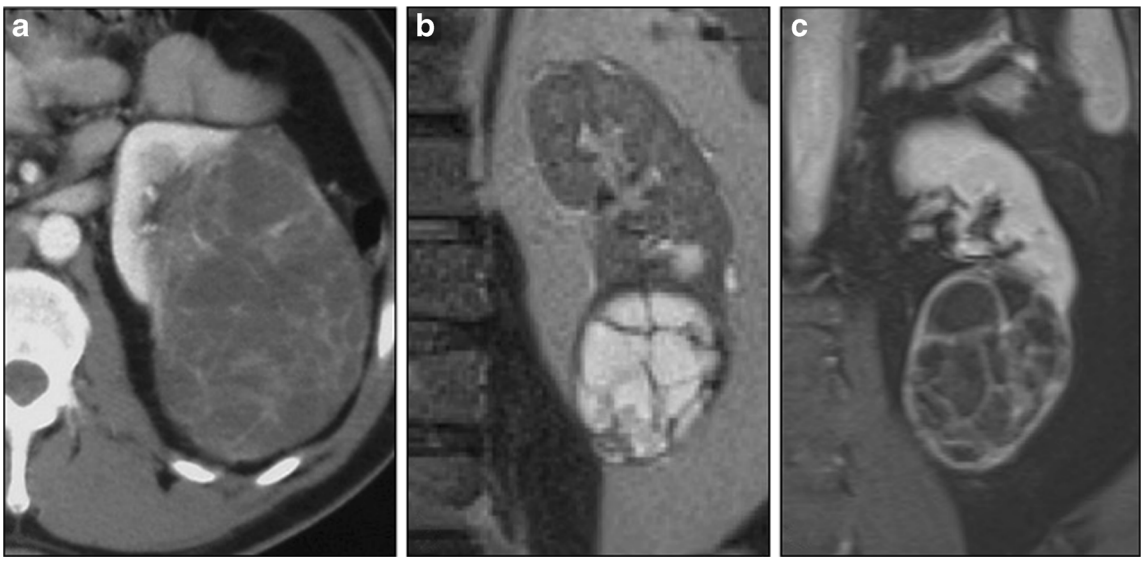

Fig. 3 Multilocular cystic renal carcinoma in a 31-year-old HIV-positive male patient with left flank pain. Contrast-enhanced CT axial (**a**) images demonstrate a large cystic mass with multiple internal septations. Different case of a 49-year-old female with left flank discomfort. Single shot fast spin echo gradient T2-weighted coronal (**b**) and T1-weighted contrast enhanced fat suppression (**c**) images show a round cystic mass with multiple internal enhancing thick septations

differentiate MCRCC from other cystic lesions. Cystic renal masses that should be in the differential diagnosis are primarily cystic nephroma, extensively cystic clear cell RCC (cRCC), clear cell variant of papillary RCC, cystic necrosis in RCC, tubulocystic carcinoma, and mixed epithelial stromal tumor [16, 17, 20]. However, the principal differential diagnosis is low nuclear grade clear cell RCC with extensive cystic changes [15].

MCRCC is a low-grade tumor with slow indolent growth and excellent prognosis, which can be cured surgically with nephrectomy or partial nephrectomy and recurrence and metastatic disease have not been reported [16, 17, 19, 20].

Mucinous Tubular and Spindle Cell Carcinoma

Mucinous tubular and spindle cell carcinoma (MTSCC) is a rare renal epithelial carcinoma recognized in 2004 in the WHO classification of adult renal epithelial neoplasms [21]. Conversely to other renal neoplasms, MTSCC has a female predilection and usually affects the adult population and present at a mean age of 53 [22].

This is well-circumscribed encapsulated tumor, frequently confined to the kidney arising from the distal nephron, specifically from the Loop of Henle [9]. Histologically, exhibits three morphologic elements: tubules, spindle cells, and extracellular mucinous/myxomatous stroma [22]. Tubules are elongated, lined by small cuboidal cells, and separated by mucinous or myxoid stroma. The spindles cells are low-grade epithelial cells. On immunohistochemical analysis is positive for vimentin, cytokeratin 7, CD10, and p504S [23]. Chronic inflammation, foamy cells, and hemorrhagic or necrotic foci are uncommon [9].

On imaging, MTSCC usually presents as a solitary well-defined exophytic or partially exophytic mass localized in the medullary region with an expansive growth pattern [5, 24]. The tumor is seen as regular iso-attenuated or hypoattenuated mass on plain CT imaging [5, 25]. On contrast-enhanced CT, exhibits low enhancement pattern in the corticomedullary phase (Fig. 4), greater enhancement degree in the excretory phase, and maximum enhancement in the nephrogenic phase [23]. Lesions smaller than 5 cm are homogenously enhanced while an heterogenous enhancement pattern is seen in lesions greater than 5 cm [22]. On MRI, MTSCC are heterogeneously iso-to-hyperintense on T2-weighted images due to the mucinous or myxomatous stroma components of the tumor. Central high signal intensity foci in T2-weighted images may correlate with edema, hemorrhage, or necrosis. On contrast MRI, the tumor exhibits the same progressive enhancement pattern on late phases seen on contrast CT imaging [24].

This renal neoplasm is a low-grade malignancy with favorable prognosis when on presence of typical morphology. However, MTSCC with sarcomatoid dedifferentiation and high nuclear grade present a more aggressive behavior with greater risk for metastatic disease, usually to regional lymph nodes, lungs, and bones [25]. Localized tumors are treated with partial or radical nephrectomy or percutaneous ablation therapy. Treatment guidelines for metastatic disease is not well established; however, there are some literature reporting response to sunitinib [22].

Fig. 4 Mucinous tubular and spindle cell carcinoma in a 64-year-old male with history of diabetes and hypertension, complaining of left flank pain. Contrast-enhanced CT axial (**a**) image show fluid filled lobulated cavities with coarse large calcifications in the left kidney mimicking hydronephrosis

Renal Oncocytoma

Renal oncocytoma is a rare benign cortical renal tumor that account for 3% to 5% of renal epithelial neoplasms in adults [5]. Affects more commonly the male population with a mean age of 65 years and most cases have an asymptomatic clinical course [26••].

Oncocytomas arise from intercalated tubular cells of the collecting tubules. Macroscopically, a central scar is a feature of oncocytoma; however, it is not specific and is only present in 33% of the cases. Chromophobe renal cell carcinoma can also present a central scar [26••]. Histologically, they are compromised by oncocytes which are polygonal or round-shaped cells organized on acini and nests with eosinophilic granular cytoplasm surrounded by a hyalinized or edematous myxoid stroma with thin capillaries [27, 28•].

Oncocytoma is commonly a solitary mass, however can manifest bilaterally in 5% and be multifocal in 13% of the cases. On ultrasound, oncocytoma shows echogenicity similar to renal parenchymal or slightly hyperechoic with the central scar seen as a hypoechoic area [29]. On CT imaging, it is seen as a well-circumscribed mass, small

tumors exhibit a homogenous contrast enhancement and conversely tumors larger than 3 cm are usually heterogeneously enhanced (Fig. 5). On T1-weighted images, low signal intensity and high signal intensity on T2-weighted images can be seen. In about 50% of the cases, a hypointense capsule may be seen; however, RCCs can also have this well-defined capsule. The characteristic central stellate scar is hypointense on T1-weighted images, hyperintense on T2-weighted images, and demonstrate a stellate enhancement pattern [28•]. Multiphasic computed tomography (CT) and magnetic resonance imaging (MRI) enhancement pattern across the three phases helps to differentiate clear cell RCC from oncocytoma [30, 31].

Renal oncocytoma is a benign tumor with good prognosis, but they may demonstrate aggressive local behavior by invading the renal vein and the perinephric fat. Radical nephrectomy is the standard of care; however, partial nephrectomy may be considered in oncocytomas with classic imaging characteristics [26••, 31].

Metanephric Tumors

Metanephric Adenoma

Metanephric adenoma (MA) of the kidney is a benign neoplasm that derives from renal epithelial cells. It is a rare tumor that can present as a solid and poorly demarcated margin mass and sometimes also with calcifications and cystic features [32, 33].

This subtype of tumor can be diagnosed at any age and have a slight female predilection. Metanephric adenomas exhibit significant morphological and immunohistopathologic similarities to solid papillary renal cell carcinoma, leading to misdiagnosis. The close relation with the renal medulla can be crucial for distinguishing MA from clear cell renal cell carcinoma. MA cells are uniform, small, with high nuclear:cytoplasmic ratio, and show bland nuclei with delicate chromatin and absent or inconspicuous nucleoli [34]. Literature suggests that MA and metanephric adenofibroma arise from nephrogenic rests and represent the benign equivalents of Wilms tumor, raising concern for misdiagnosis [35].

On CT studies, MA tends to be a solitary, poorly circumscribed, hypodense, or isodense mass arising from the renal medulla with enhancement pattern lower than the cortex and rest of the medulla in all phases (Fig. 6). Since this entity is commonly asymptomatic, the tumor is usually an incidental finding. Prognosis is considered good after undergoing total nephrectomy or local resection with kidney preservation [33].

Mesenchymal Tumors

Angiomyolipoma

Angiomyolipoma (AML) is a tumor that arises from clonal proliferation of epithelioid cells distributed around blood vessels. Angiomyolipomas can also occur in other organs in association with renal angiomyolipoma. They are usually asymptomatic and can be a rare finding on a normal population, approaching 13 per 10,000 adults. However, are much prevalent in patients with pulmonary lymphangioleiomyomatosis or tuberous sclerosis, in which they are often accompanied by renal cell carcinoma [36].

Fig. 5 Renal oncocytoma in a 53-year-old female with right flank discomfort. Contrast-enhanced CT axial (**a**) coronal (**b**) and delayed phase, coronal (**c**) images show a large hypervascular mass with punctate calcifications and a central scar (arrows) involving the right kidney

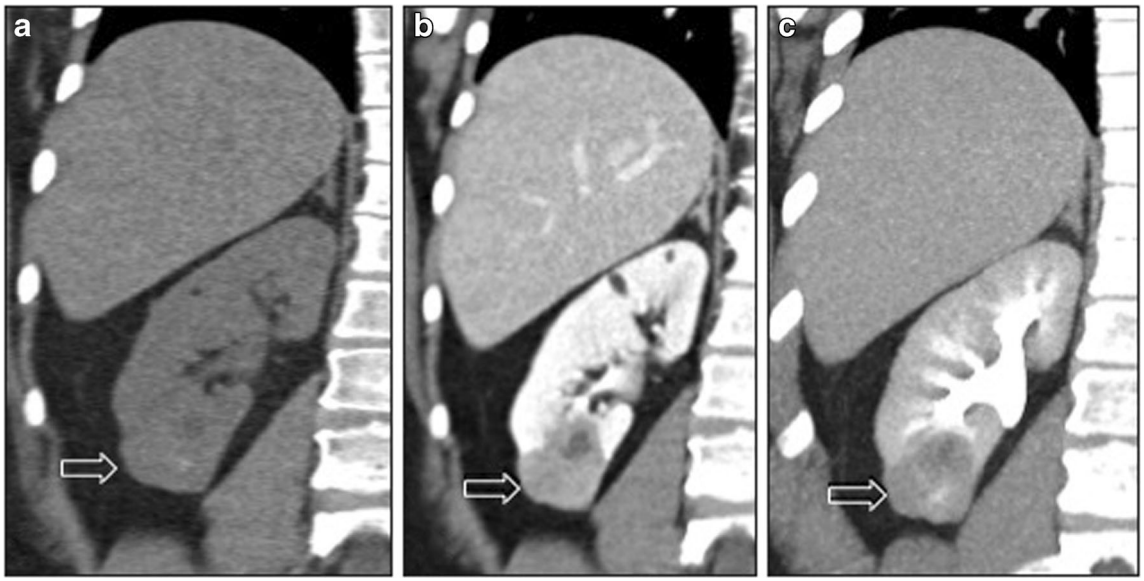

Fig. 6 Metanephric adenoma in a 27-year-old female with abdominal pain. Incidental CT finding on the right kidney. Plain CT coronal (**a**) and contrast enhanced-CT nephrographic (**b**) and delayed phases (**c**) images demonstrate a solid mass with punctate calcifications and small area of necrosis in the lower pole of the right kidney (arrows)

AML is a lesion of the kidney that expresses melanocytic markers including HMB-45 and Melan-A, and are comprised of smooth muscle–like cells, adipocyte-like cells, and epithelioid cells. It can be divided in two major histologic variants: classic type, featuring abnormally thick-walled vessels that lack a well-developed internal elastic lamina, with varied amounts of spindle smooth muscle–like cells and adipose tissue; and the epithelioid type, distinguished by the vast epithelioid cells component. The epithelioid angiomyolipoma was recently recognized as a malignant variant [37].

Typical angiomyolipomas are benign but alarming features as nuclear pleomorphism and mitotic activity, extension into the vena cava, and spread to regional lymph nodes must be evaluated. The most common complication is hemorrhage [38]. The basic feature for diagnosis on all imaging modalities is the demonstration of macroscopic fat; however, hemorrhage or atypical lesions containing little fat can be challenging when distinguishing from a renal cell carcinoma (RCC) (Fig. 7). On MRI imaging, usually AML is hyperintense in T1-weighted images due to the fat content. In T2-weighted images, high fat content tumors exhibit high signal intensity, while low fat content lesions are hypointense (Fig. 8) [28•]. Some atypical AMLs are only identified postsurgery in patients with an image suspicious for RCC [39].

Selective arterial embolization can be the treatment of choice for acute hemorrhage cases. Surgery has been recommended for lesions suspicious for malignancy or lesions bigger than 4 cm (because of increased likelihood of hemorrhage), but most typical AML radiographically diagnosed can be managed initially with surveillance or embolization [39].

Epithelioid Angiomyolipoma

Epithelioid angiomyolipoma (EAML) is an uncommon potentially malignant mesenchymal tumor. They commonly affect the kidney; however, it can occur in the lungs, liver, pancreas, bladder, prostate, genital tract, and bone [40]. EAML is highly associated with tuberous sclerosis, but it can also present without this disease [41]. They occur more commonly in females and in contrast to typical AML, affect younger population [42].

Fig. 7 An hemorrhagic angiomyolipoma in a 62-year-old female with acute abdominal pain and hypotension. Contrast-enhanced CT axial (**b**) image show a complex mostly exophytic mass with areas of fat attenuation (arrow head) and high density arising in the right kidney (arrow)

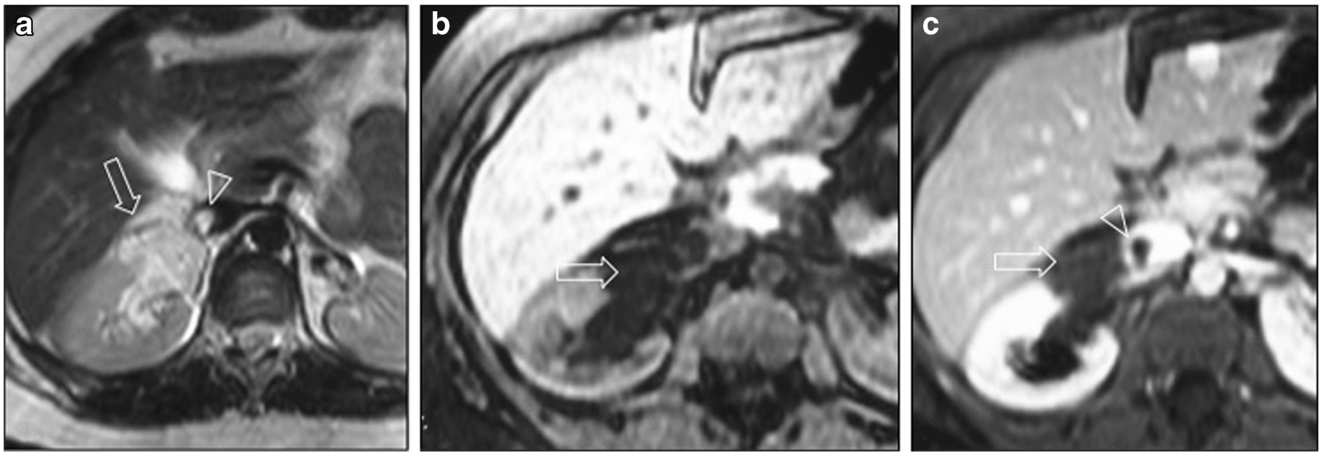

Fig. 8 Renal angiomyolipoma in T2-weighted MR axial (**a**) image is seen as a hyperintense mass in the right kidney (arrow). Fat-suppressed gradient echo T1-weighted without (**b**) and post-contrast administration (**c**) images depicts suppression of the fat in this mass (arrows). Note the extension of this tumor into the inferior vena cava (arrowheads in a and c)

EAML represents a different histological subtype of AML, by definition it is principally composed by at least 80% epithelioid cells [43]. Histologically, the epithelioid cells are arranged in sheets with abundant granular eosinophilic cytoplasm, vesicular nuclei, and prominent nucleoli and contain few or none adipocytes and vessels [41, 44].

In most cases, EAML presents as a solid ill-defined solitary mass. On non-contrast CT imaging, it is characteristically seen as an heterogenous hyperdense mass without or minimal macroscopic fat content, and in some cases central necrosis may be seen [41, 44] (Fig. 9). In cases of EAML with macroscopic fat, imaging differentiation from typical AML may be challenging and can be indistinguishable [45]. On contrast-enhanced CT imaging, they exhibit rapid wash-in and slow wash-out enhancement pattern [42]. On contrast-enhanced ultrasound (CEUS), heterogeneous early hyperenhancement in the corticomedullary phase and late iso-enhancement in the nephrographic and excretory phases have been reported [46].

On MRI, it is seen as a large exophytic mass with low-signal intensity on T2-weighted images and may demonstrate macroscopic or microscopic fat with enlarged vessels and hemorrhagic areas [44, 47].

The mainstay of treatment is radical nephrectomy and neoadjuvant or adjuvant targeted therapy with Everolimus to inhibit the mTOR pathway may be considered [48]. In contrast to AML, EAML presents a more aggressive behavior; it can locally extend or invade the renal vein, inferior vena cava, or regional lymph nodes; it may recur after surgical resection or present distant metastasis, more frequently to lungs and liver [28•, 41]. The degree of epithelioid cell atypia, high and atypical mitotic activity, and presence of necrosis are highly associated with aggressive clinical behavior [43, 45, 48].

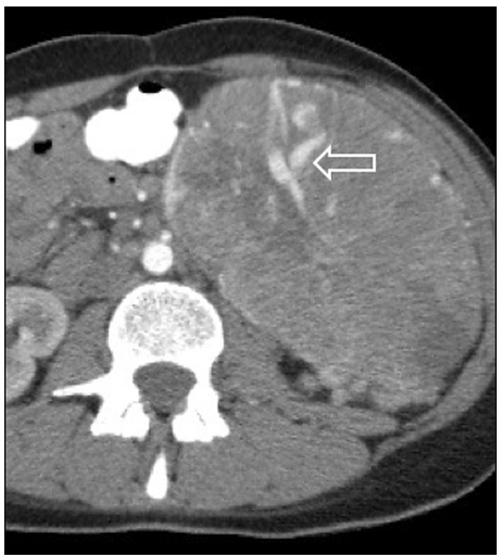

Fig. 9 Epithelioid angiomyolipoma in a 33-year old female with a left abdominal mass. Contrast-enhanced CT axial image show a heterogeneous solid mass with large internal tortuous vessels (arrow) involving the left kidney

Inflammatory Myofibroblastic Tumor/Inflammatory Pseudotumor

Inflammatory myofibroblastic tumor (IMT) is a rare benign type of myofibroblastic tumor, given that exhibits clinical and imaging features similar to malignant neoplasms it is also known as inflammatory pseudotumor. IMT is more common in males and it can affect young and adult population. This tumor can affect almost any organ; however, it frequently occurs in lungs, retroperitoneum, hepatobiliary tract, gastrointestinal tract, head and neck, and rarely in the urogenital tract and soft

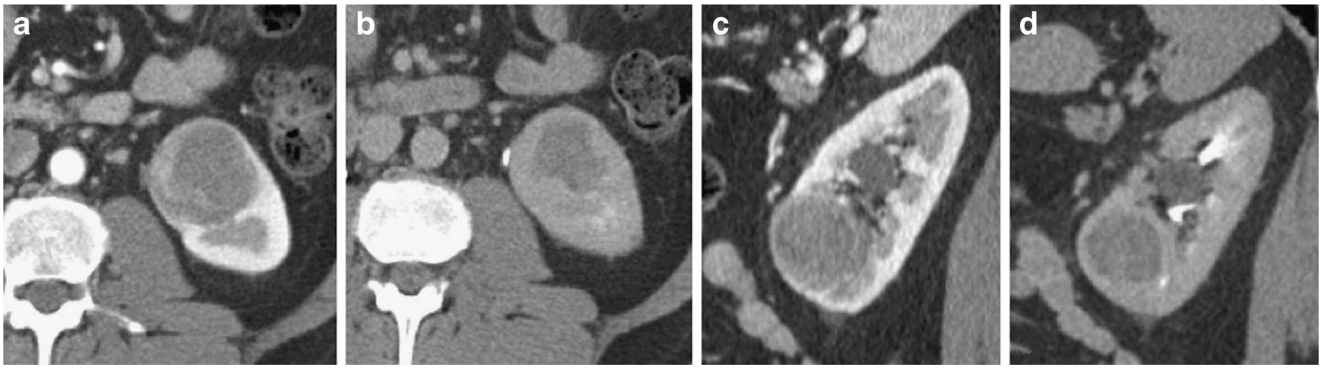

Fig. 10 Inflammatory pseudotumor (myofibroblastic tumor) in a 62-year-old male with left flank pain and hematuria. Contrast-enhanced CT axial, arterial (**a**) and delay (**b**) phases and sagittal arterial (**c**) and coronal (**d**) images reveal a hypoattenuated mass with irregular focal wall thickening in the lower pole of the left kidney

tissues [49–51]. The urethra and the bladder are the most common sites affected in the urogenital tract, and it is extremely rare that it arises in the kidney [52].

Histologically, it is a tumor comprised of differentiated myofibroblastic spindle cells, with inflammatory cells infiltration with lymphoplasmacytic infiltrates and myxomatous stroma. On immunohistochemical analysis, it demonstrates expression for vimentin and smooth muscle actin [49, 53].

On ultrasound, IMT is seen as a hypoechoic renal mass and may demonstrate regular or irregular borders. On Doppler, it may show increased vascularity [51]. On CT imaging, it is a homogenous or heterogenous hypodense renal mass (Fig. 10). On MRI, it is iso-intense on T1-weighted images and exhibits iso-to-low-signal intensity on T2-weighted images. After contrast administration, it demonstrates heterogenous enhancement pattern on CT and MRI imaging, likely due to its fibrous content [49, 51, 53]. The standard of care is radical or partial nephrectomy and local recurrence and metastatic disease can be seen in some cases [53, 54].

Renal Rhabdomyosarcoma

Rhabdomyosarcoma (RMS) is the most common soft tissue sarcoma in pediatrics, representing 5% to 10% of all solid tumors in children [55–57]. Primary renal RMS on the other hand is considered extremely rare and has aggressive features like other primary renal sarcomas [58].

RMS can be classified into four major groups, according to the WHO: embryonal RMS (ERMS), alveolar RMS (ARMS), pleomorphic RMS (PRMS), and spindle cell/sclerosing RMS (SRMS) [59]. There are two subsets of embryonal RMS: standard histology and botryoid histology. In children, renal pelvic involvement raises a bigger possibility of a primary RMS [60]. Grapes appearance of the tumor in the renal pelvis should raise the suspicion of embryonal renal rhabdomyosarcoma. Review of the literature revealed only 23 cases of primary renal RMS. Most of the reported cases consist of embryonal type and other few are of pleomorphic and alveolar subtype or undifferentiated sarcomas [59].

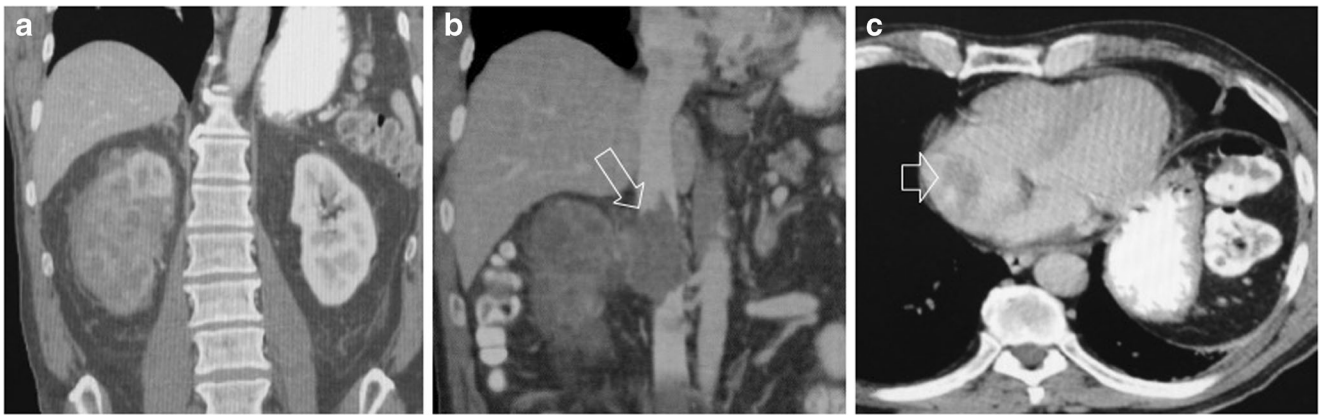

Fig. 11 Renal rhabdomyosarcoma in a 71-year-old male with hematuria and shortness of breath. Contrast-enhanced CT coronal arterial (**a**) and venous (**b**) phases images demonstrate an infiltrative low attenuation mass involving most of the right kidney and extending into the lumen of the inferior vena cava (arrow). Contrast-enhanced CT axial (**c**) image of the chest, reveal the presence of a tumor thrombus in the right atrium (arrowhead)

On imaging, renal rhabdomyosarcoma may appear as a well-defined expansile mass or as a diffuse infiltrative mass. However, its imaging characteristics are not specific and indistinguishable from RCC, renal adenocarcinomas, or other sarcomas (Fig. 11) [8].

Treatment of rhabdomyosarcoma involves complete resection with margin consisting of 0.5 cm circumferentially or an uninvolved fascial margin. Children with rhabdomyosarcoma usually present with localized disease, and with the current multimodality treatment protocols, a cure rate of more than 70% can be achieved [57].

Ewing Sarcoma

Ewing sarcoma comprises 10–15% of all bone sarcomas and is the second most common malignant tumor of the bone. On the other hand, primary Ewing sarcoma (PES) of the kidney, first described in 1975 by Seemayer et al., is an extremely rare entity, with isolated case reports documented on the literature [61].

PES of the kidney belongs to the family of primitive neuroectoderm tumors (PNETs). Translocation of *t*(11;22)(q24;q12) in cases of Ewing's sarcoma, PNET, and Askin's tumor support the hypothesis that these tumors are related. Histologic features are small round cells with high nuclear to cytoplasmic ratios that are arrayed in sheets [62].

It is usually an aggressive tumor which usually occurs in young adults between 20 and 30 years old. Males are more affected on a ratio of 3:1 (male:female) [63]. Clinical features are usually abdominal/flank pain or hematuria. Computed tomography usually shows renal masses and areas of necrosis and hemorrhage (Fig. 12).

The diagnosis is made based with immunohistochemical markers CD99, FLI-1, and WT1. Other small blue round cell tumors must be ruled out before making the diagnosis. PES of the kidney typically has poor response to therapy, with a 5-year disease-free survival of 45% to 55% [64–66].

Mixed Epithelial and Stromal Tumors

Mixed Epithelial and Stromal Tumor

First described by Michal and Syrucek in 1998, this tumor of the kidney is composed of a mixture of stroma and epithelium with solid and cystic architecture. It has been also previously described under many other nomenclatures because of the big spectrum of this entity [67].

Mixed epithelial and stromal tumor (MEST) usually presents in perimenopausal woman around 45 years old with nonspecific urinary symptoms. This neoplasm is biphasic and has both epithelial and spindle cell elements; the epithelial feature consists of clusters of tubules lined by flattened to cuboidal epithelium plus eosinophilic cytoplasm and a hobnail appearance; the mesenchymal portion usually resembles ovarian stroma [21, 68].

On CT imaging, MEST can present as a well-circumscribed, multiseptated cystic and solid mass with delayed contrast material enhancement (Fig. 13). Since it is a rare entity, features of MEST on ultrasound and magnetic resonance are poorly described, with a few cases in which appeared as a heterogeneous hyperechoic mass at US and as a solid and cystic mass with heterogeneous enhancement on MR imaging [69]. Most of these tumors have a benign progression, but rare malignant transformation has been reported in the literature. Therefore, intraoperative frozen section may be performed to a margin assessment, when a partial nephrectomy is in course.

Multilocular Cystic Nephroma

Multilocular cystic nephroma (MLCN) is a benign slow-growing tumor of the kidney and is considered infrequent within the renal tumors spectrum. According to Gallo and Pechansky, multilocular cystic nephroma can be found in 2.4% of the primary renal tumors [70].

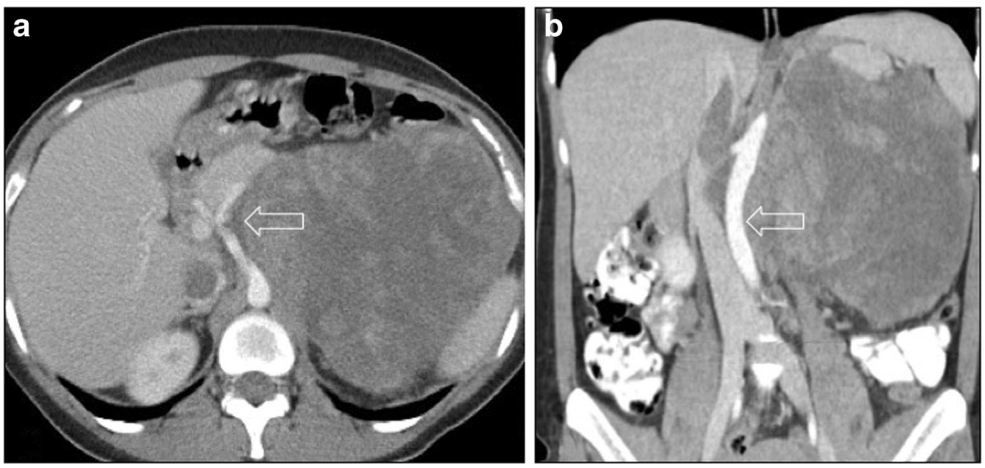

Fig. 12 Ewing's sarcoma of the kidney in a 29-year-old female with abdominal pain. Contrast-enhanced CT axial (**a**) and coronal (**b**) images show a large heterogeneous solid mass involving most of the left kidney. Note the mass effect of this mass in the celiac and mesenteric arteries and abdominal aorta (arrows)

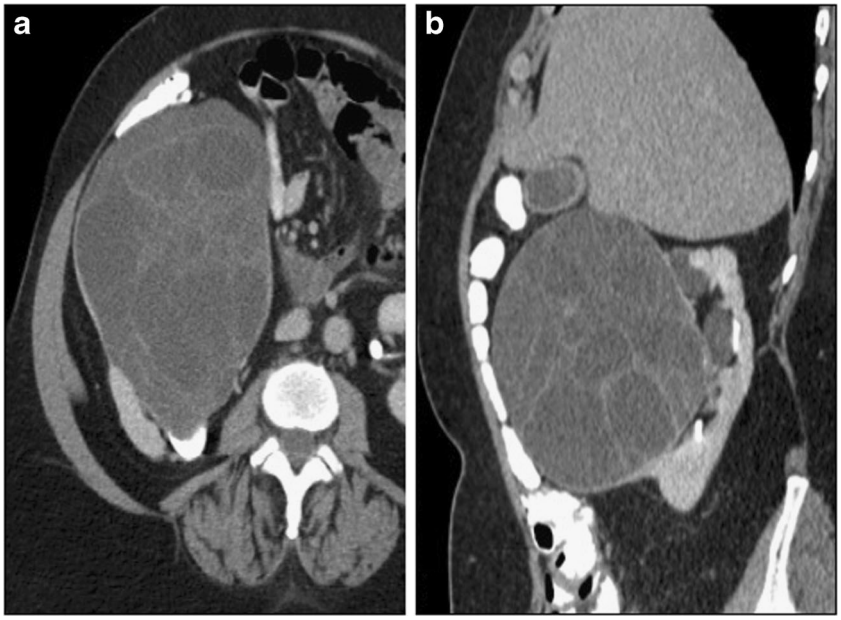

Fig. 13 Mixed epithelial and stromal tumor (MEST) in a 32-year old female with right flank discomfort. Contrast-enhanced CT axial (**a**) and sagittal (**b**) images show a large cystic mass in the right kidney with multiple internal septations compressing the collecting system

Nonspecific urinary tract symptoms in the adult and abdominal mass in the child are the most common symptoms of the disease. It is considered a mixed epithelial-stromal tumor of the kidney that most often occur in young children and adults in middle age, with a predominance of males and postmenopausal women [71].

They are typically well-circumscribed by a thick, fibrous capsule on gross inspection and can compress the adjacent renal parenchyma. The disease can be misinterpreted as aggregates of simple retention cyst, multicystic kidney, or polycystic disease. However, typical epithelial lined cystic spaces and mesenchymal stroma are invariably present on MLCN tumors [72].

Radiology is imperative in guiding the diagnostic process. MLCN presents as a unilateral mass with irregular cysts and septa of variable thicknesses. The findings usually correspond to a category III Bosniak classification of renal cystic masses. To suggest a benign disease, the absence of solid components and vascular abnormalities and the presence of homogeneous renal parenchyma must be present. On CT, MLCN appears as a well-circumscribed cystic mass with several hypoattenuated components and no contrast excretion into the cystic components (Fig. 14) [71].

The possibility of multilocular cystic renal cell carcinoma cannot be definitely excluded without histologic analysis, therefore surgery must be indicated. Because of its benign nature, this lesion can be best managed by a nephron sparing surgery. Long-term follow-up is encouraged even with lack of literature evidence of local recurrence or metastatic disease [73].

Miscellaneous Tumors

Wilms Tumor

Wilms' tumor accounts for 6% of all pediatric malignancy and is the most common renal tumor in kids with an overall annual incidence of 8.1 per million children in North America [74].

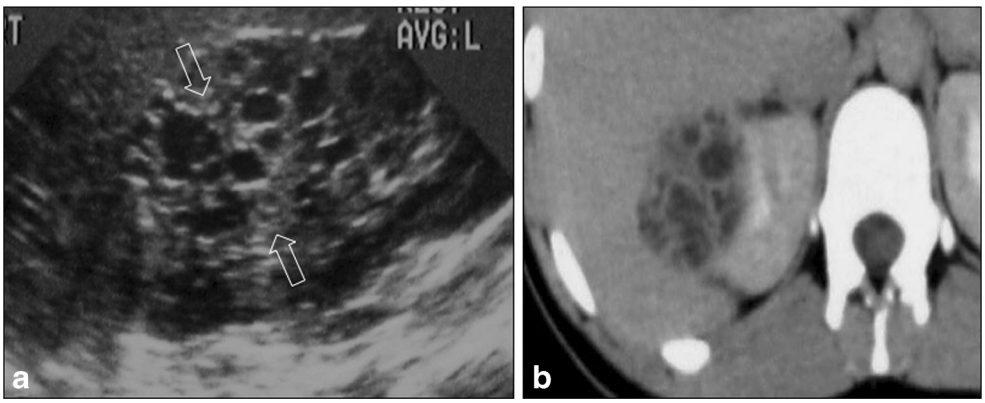

Fig. 14 Multilocular cystic nephroma in a 18-year old female with right flank pain. Ultrasound sagittal (**a**) shows a multiseptated mass in the right kidney (arrows). Contrast-enhanced CT axial (**b**) image demonstrate the presence of a complex multiseptated mass in the upper pole of the right kidney

One-third of the cases can be associated with either singly or in combination mutations of Wilms tumor 1 (WT1), Wilms tumor gene on the X chromosome (WTX; also known as FAM123B and AMER1), β-catenin (CTNNB1), and TP53 [75]. Wilms tumor can also occur as a part of a multiple malformation syndrome in approximately 10% of cases, including WAGR, Denys-Drash, and Beckwith-Wiedemann syndromes [76]. High-risk patients should be screened with serial abdominal ultrasonography [77].

Wilms tumor is typically surrounded by a pseudocapsule and may include cysts, hemorrhage, or necrosis. Histologically, Wilms tumor is comprised of three cell types: blastemal cells (undifferentiated cells), stromal cells, and epithelial cells. Anaplasia is associated with poor outcome [78].

On imaging, Wilms tumor is seen heterogeneously echogenic on ultrasound. On CT imaging, it may appear as a heterogenous solid mass with calcifications and fat (Fig. 15). On MRI, it is hypointense on T1-weighted images and hyperintense on T2-weighted images [79].

Ninety-five percent of cases are diagnosed by 10 years of age. Bilateral tumor cases present ~ 12 months earlier than unilateral cases and are rarer. Only a few cases of nephroblastoma in adults have been described in literature (about 3% of all described cases), making it a rare condition [80, 81].

National Wilms Tumor Study is a staging system based upon surgical evaluation prior to the administration of chemotherapy [82]. Patients with advance disease can undergo an upfront biopsy and receive nephrectomy chemotherapy [83]. The discovery of the tumor's radiosensitivity and chemotherapy agents has resulted in a striking improvement in survival rate to 90% [82].

Renal Teratoma

Teratoma is a germ cells neoplasm that arises from pluripotent cells and can differentiate into other embryonic germ lines. The component tissues of this type of tumor can range from immature to well differentiate and are foreign to the anatomic site in which they are found. They commonly arise in the gonads and the predominant extragonodal location is the retroperitoneum, making the renal teratoma an extremely rare condition [84].

The majority of the renal teratomas are known to occur in childhood; even more uncommon is their presentation in adults [85]. Only a few cases of renal teratoma have been described in literature. Majority of these cases could either be a Wilm's tumor with teratoid features or a renal extension of retroperitoneal teratoma [86]. Teratomas are usually solid and avascular but a cystic teratoma may be confused with cystic lesions of the kidney [87].

On CT imaging, teratomas are heterogenous solid or mixed solid-cystic masses with calcifications and low-density areas corresponding to fat (Fig. 16). On MRI, cystic components demonstrate low signal intensity on T1-weighted images and high signal intensity on T2-weighted images. Teratomas may show peripheral high signal intensity foci on T1-weighted images and low signal intensity on T2-weighted images which correlate with proteinaceous or hemorrhagic components.

The majority of patients have a benign clinical course; however, it is difficult to assess the natural history of teratoma occurring in adults because metastatic spread from well-differentiated extrarenal teratomas has been observed in some cases, leading to worsening of prognosis. Therefore, hence complete excision is totally justified. A thorough search for an extrarenal source of the RT is imperative, regardless of the histologic maturity of the elements of the tumor.

Renal Lymphoma

Primary renal lymphoma is very rare; it accounts to less than 1% of extra nodal lymphomas, but kidneys are the most common affected organ of extra nodal involvement.

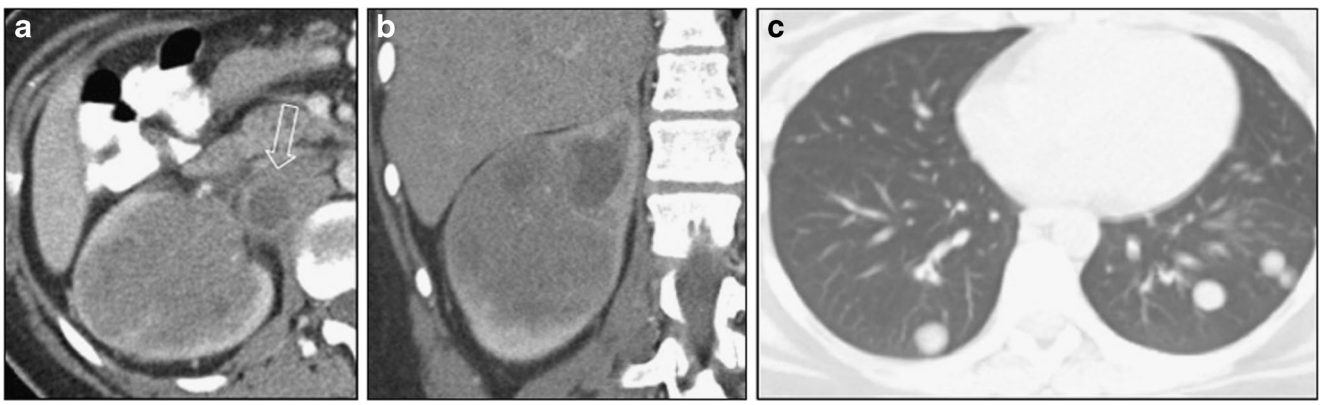

Fig. 15 Wilms tumor in a 21-year-old female with right flank pain. Contrast-enhanced CT axial (**a**) and coronal (**b**) images demonstrate a large hypoattenuating solid mass involving the right kidney. Note the extension of this tumor into the inferior vena cava (arrow). Axial chest CT image (**c**) reveals multiple pulmonary metastases

Fig. 16 Renal teratoma in a 58-year-old female complaining of abdominal pain. Contrast-enhanced CT coronal image show a small mass of low attenuation with coarse calcifications (arrow) in the lower pole of the right kidney

Secondary lymphoma renal involvement usually results from hematogenous spread or contiguous extension from retroperitoneal lymph nodes [26••, 88]. Frequently affects immunocompromised population, and the more common types are large B cell non-Hodgkin lymphoma and Burkitt lymphoma [89].

Grossly is a fleshy, firm, yellow to gray tumor presenting as solitary or multiple masses, with perinephric extension or with local or diffuse kidney infiltrative disease [13, 26••].

Large masses present central hemorrhage and necrosis. Histological features include uniform cells with prominent nuclei and scant cytoplasm. Burkitt lymphoma shows uniform medium basophilic cells with clear histiocytes giving the classic "starry sky" pattern [14••].

On imaging, lymphoma commonly presents as multiple bilateral homogenous masses with hypoechoic appearance on US imaging with posterior acoustic enhancement, and can be easily confused with renal cysts [8]. On CT imaging, it demonstrates low attenuation and a weak enhancement after contrast administration (Fig. 17). On T1- and T2-weighted images, it has low to intermediate signal intensity and high signal intensity on DWI. After gadolinium administration, it shows less enhancement than the renal parenchyma; however, on delayed phase, some lesions may exhibit progressive enhancement [14••, 89, 90]. Less commonly may present unusual imaging findings like necrosis, cystic changes, hemorrhage, and calcifications. PET/CT is the modality of choice for staging and treatment response evaluation [8, 90].

The main stay of treatment of a renal mass is nephrectomy; however, renal lymphoma is treated with chemotherapy with cyclophosphamide, hydroxydaunorubicin, oncovin, and

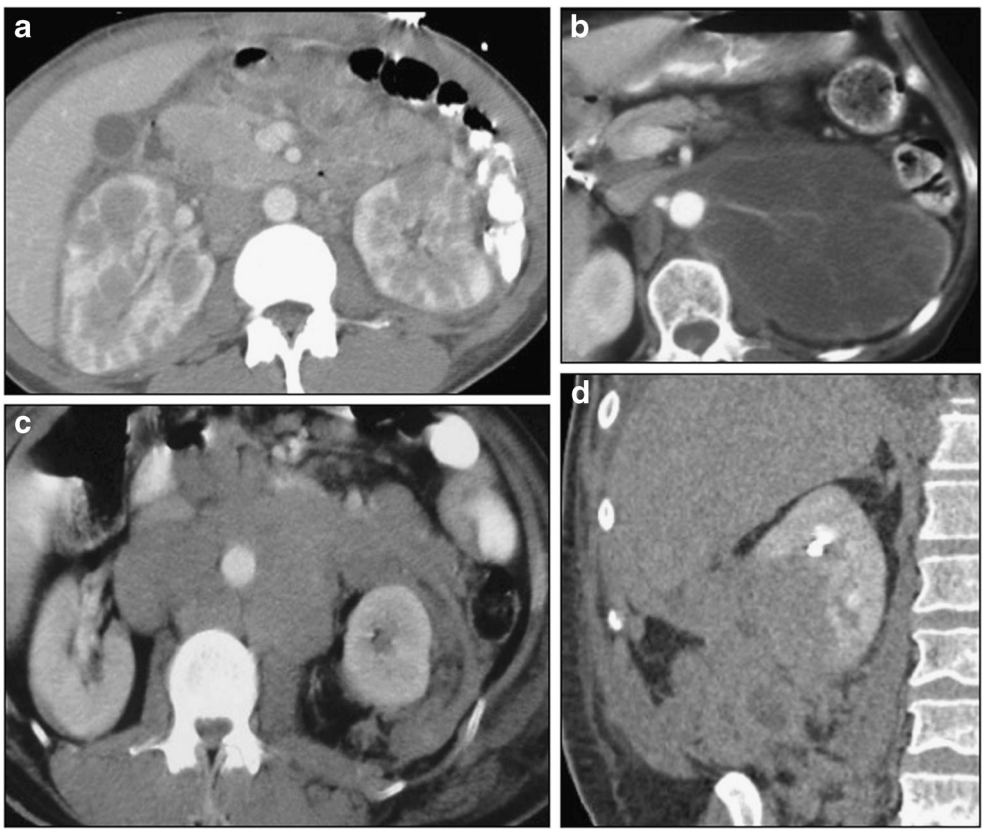

Fig. 17 Spectrum of imaging appearances of renal lymphoma on contrast-enhanced CT axial images. Renal lymphoma may present with enlarged kidneys with multiples round hypoattenuated masses (**a**) or as a hypoattenuated mass with diffuse infiltration of the renal parenchyma (**b**). In other cases, it can present as a perirenal soft mass associated with multiple retroperitoneal nodes (**c**) or as a perirenal mass extending into the renal parenchyma as seen in this coronal image (**d**)

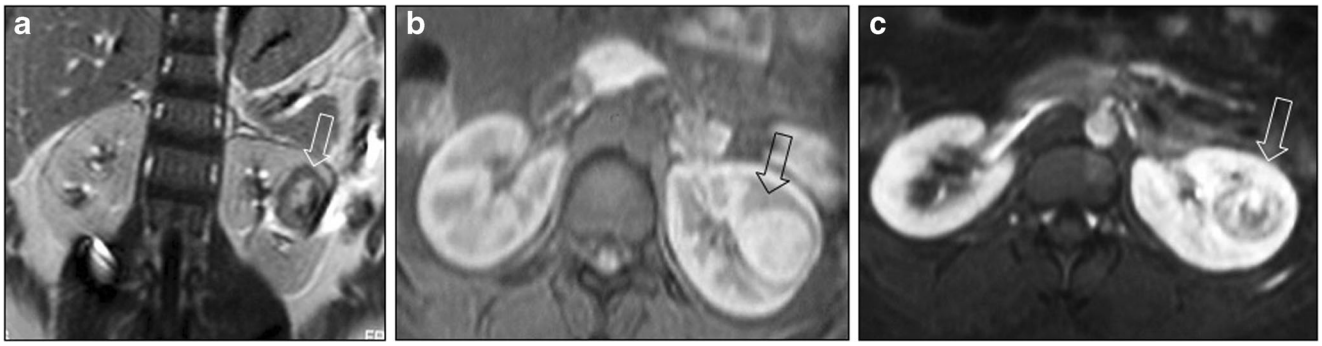

Fig. 18 Renal gastrinoma in a 24-year-old male with intractable duodenal ulcers. An incidental mass in the left kidney was found by MR. Single shot fast spin echo T2-weighted coronal (**a**) and fat-suppressed T1-weighted image after the administration of intravenous contrast arterial (**b**) and delayed (**c**) images demonstrate a round heterogeneous hypervascular mass with a thick capsule in the left kidney (arrows)

prednisone (CHOP) regimen with rituximab for CD20-positive non-Hodgkin lymphoma. Primary renal lymphoma is a malignancy with very poor prognosis with 1-year mortality rate of 75% [8, 91].

Metastatic Tumors

Renal Gastrinoma

Gastrinomas are the most common cause of Zollinger-Ellison syndrome and are usually found at the gastrinoma triangle. It is also highly associated with multiple endocrine neoplasia type 1 (MEN-1) and can be multicentric. Ectopic gastrinoma have been reported in the literature; however, renal gastrinoma is an extremely rare disease with only few cases described [92, 93]. Immunocytochemical analysis reveals gastrin-positive tissue. Somatostatin receptor scintigraphy is a sensitive method for detection of the tumor in patients with hypergastrinemia. A selective renal vein gastrin assay may be used to establish the diagnosis in difficult cases, in addition to renal mass findings on CAT scan [93]. On CT imaging, it can present a central hypodense area, but because of the lack of typical radiographic and cytological findings, preoperative diagnosis is impossible in most cases (Fig. 18). However, this diagnosis should be considered in all patients with high gastrin levels and a solid mass in the kidney [93].

Metastases to the liver are frequent finding for sporadic gastrinomas outside the gastrinoma triangle supporting the notion that these gastrinomas behave differently from those found within the gastrinoma triangle. This is based on the theory that a fetal cell is present in the adult and is being implicated in tumor (gastrinoma) formation. Nephrectomy is usually curative in this type of tumor [93, 94].

Renal Metastasis

Metastatic disease to the kidney is the most common renal malignancy with a reported prevalence of 48% in autopsy studies of patients who died secondary to a malignancy cause. Renal metastases represent the fifth most affected organ from hematogenous spread [95]. About 2–5% of small renal masses are metastasis from a non-renal primary malignancy [96].

Primary tumors that most commonly metastasize to the kidney are lung (Fig. 19), breast, gastrointestinal tumors, and melanoma and less commonly female genital tract, head and neck, colon (Fig. 20), and prostate cancers [26••, 95].

Usually, renal metastases present as multiple or bilateral ill-defined lesions with infiltrative growth pattern usually in the zone between the renal cortex and medulla. Infrequently, they present as solitary lesions with exophytic pattern, which may be confused with RCC [26••, 95, 97].

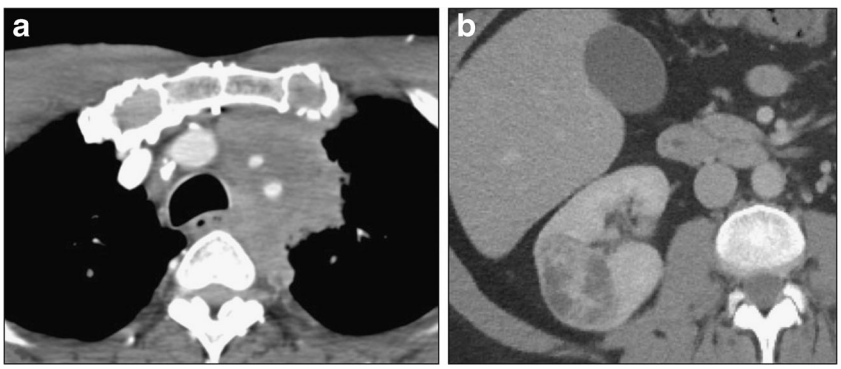

Fig. 19 Renal metastasis form small cell carcinoma of the lung. Contrast-enhanced CT axial (**a**) of the chest and abdomen images reveal a soft tissue mass in the left upper lobe involving the mediastinum and encasing the adjacent vessels (**a**) and a heterogeneous well-circumscribed mass involving the right kidney (**b**)

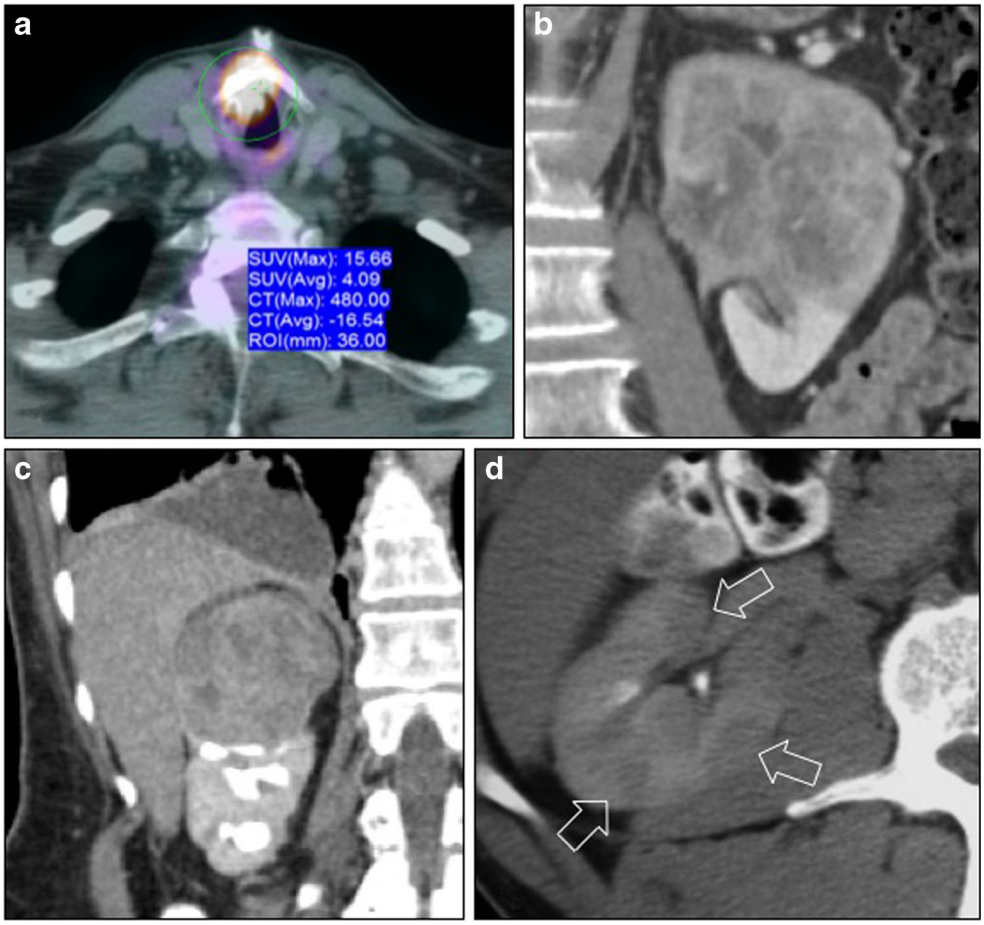

Fig. 20 Renal metastases from squamous cell carcinoma of the larynx. Fused PET/CT axial (**a**) image shows intense FDG uptake in a laryngeal mass. Contrast-enhanced CT coronal (**b**) image demonstrate a large infiltrative mass involving the upper pole of the right kidney. Renal metastases from granulosa cell tumor of the ovary. Contrast-enhanced CT coronal (**c**) image demonstrate a heterogenous mass involving the upper pole of the right kidney. Renal metastases from colon carcinoma. Contrast-enhanced CT axial (**d**) images reveal multiple low attenuation masses involving the right kidney (arrows)

On CT imaging, they exhibit low attenuation in comparison to the renal parenchyma; however, metastases from melanoma and breast cancer may be hypervascular [95, 97]. CT is a very useful and sensitive imaging modality for detection of renal metastases, given its capability to detect small renal masses, metastatic extension evaluation, and enhancement characterization [98].

Percutaneous biopsy must be considered in a renal mass for histologic confirmation to differentiate a primary renal tumor from renal metastatic disease in order to determine the appropriate treatment [99].

Others Tumors

Renal Sarcoid Mass

Sarcoidosis is a multisystem granulomatous disorder characterized by the presence of noncaseating granulomas and affects mainly the lungs. It typically occurs in young adults and can involve all organ systems to a varying extent and degree. Extrapulmonary sarcoid can be present up to 30% of patients [100].

Fig. 21 Renal sarcoid in a 48-year-old African-American patient with hypertension and hepatosplenomegaly. Contrast-enhanced CT axial (**a**, **b**) images reveal multiple small lesions of low attenuation involving the liver and the spleen (**a**). In addition, a large heterogeneous mass in the left kidney (**b**) (arrow). Histologic analysis (**c**) revealed noncaseating granulomas consistent with sarcoid

Pseudotumoral renal sarcoidosis is a rare tumor and can present diversified imaging features. Ultrasound imaging was documented as both hyper- and hypoechoic patterns as well as enhancing and non-enhancing masses on CT (Fig. 21). They can also present not only as a single rounded mass but also as multiple wedge-shaped lesions on CT [101].

The diagnosis of sarcoidosis is supported by histologic findings. It is usually a diagnosis of exclusion, since noncaseating granulomas with epithelioid cells and large, multinucleated giant cells are features found in other inflammatory processes such as tuberculosis, histoplasmosis, and fungal infections [102].

There are reports on the literature of that resolution of radiologic findings were found with the use of continued prednisone therapy. However, there are no evidence-based findings to support the therapy except for renal function maintenance [102]. It is essential that radiologist be attentive of sarcoid lesions of the kidney in individuals with a renal mass because treatment can change substantially.

Conclusion

Renal masses are a common finding in clinical practice. Detection of these masses has increased in the last years, yet mortality rates have slightly decreased. A considerable variety of particular tumors can arise from the kidney, challenging the expertise of radiologists and urologists on this subject. Histopathological analysis should always be assessed for final diagnosis of these tumors. However, imaging can be an important diagnostic guidance until therapy of choice. Clinical and imaging features can include differential diagnosis and must always be assessed for better patient treatment. The awareness of these unusual entities is vital for professionals working at a complex medical facility with greater volume of patients.

Compliance with Ethical Standards

Conflict of Interest R. Patricia Castillo, Juan F. Santoscoy, Leonardo Pisani, Beatrice L. Madrazo, and V. Javier Casillas each declare no potential conflicts of interest.

Human and Animal Rights and Informed Consent This article does not contain any studies with human or animal subjects performed by any of the authors.

Publisher's Note Springer Nature remains neutral with regard to jurisdictional claims in published maps and institutional affiliations.

References

Papers of particular interest, published recently, have been highlighted as:
- • Of importance
- •• Of major importance

1. Campbell S, Uzzo RG, Allaf ME, Bass EB, Cadeddu JA, Chang A, et al. Renal mass and localized renal cancer: AUA guideline. J Urol. 2017;198(3):520–9.
2. O'Connor SD, Pickhardt PJ, Kim DH, Oliva MR, Silverman SG. Incidental finding of renal masses at unenhanced CT: prevalence and analysis of features for guiding management. Am J Roentgenol. 2011;197(1):139–45.
3. Moch H, Cubilla AL, Humphrey PA, Reuter VE, Ulbright TM. The 2016 WHO classification of tumours of the urinary system and male genital organs—part a: renal, penile, and testicular Tumours. Eur Urol. 2016;70(1):93–105.
4. Kobayashi N, Matsuzaki O, Shirai S, Aoki I, Yao M, Nagashima Y. Collecting duct carcinoma of the kidney: an immunohistochemical evaluation of the use of antibodies for differential diagnosis. Hum Pathol. 2008;39(9):1350–9.
5. Wu J, Zhu Q, Zhu W, Chen W, Wang S. Comparative study of CT appearances in mucinous tubular and spindle cell carcinoma and collecting duct carcinoma of the kidney. Br J Radiol. 2015;88(1056):20140434.
6. Gupta R, Billis A, Shah RB, Moch H, Osunkoya AO, Jochum W, et al. Carcinoma of the collecting ducts of bellini and renal medullary carcinoma: clinicopathologic analysis of 52 cases of rare aggressive subtypes of renal cell carcinoma with a focus on their interrelationship. Am J Surg Pathol. 2012;36(9):1265–78.
7. Tokuda N, Naito S, Matsuzaki O, Nagashima Y, Ozono S, Igarashi T. Japanese Society of Renal Cancer. Collecting duct (Bellini duct) renal cell carcinoma: a nationwide survey in Japan. J Urol. 2006;176(1):40–3.
8. Prasad SR, Humphrey PA, Menias CO, Middleton WD, Siegel MJ, Bae KT, et al. Neoplasms of the renal medulla: radiologic-pathologic correlation. Radiographics. 2005;25:369–80.
9. Prasad SR, Humphrey PA, Catena JR, Narra VR, Srigley JR, Cortez AD, et al. Common and uncommon histologic subtypes of renal cell carcinoma: imaging spectrum with pathologic correlation. Radiographics. 2006;26(6):1795–806.
10. Beckermann KE, Sharma D, Chaturvedi S, Msaouel P, Abboud MR, Allory Y, et al. Renal medullary carcinoma: establishing standards in practice. J Oncol Pract. 2017;13(7):414–21.
11. Sirohi D, Smith SC, Ohe C, Colombo P, Divatia M, Dragoescu E, et al. Renal cell carcinoma, unclassified with medullary phenotype: poorly differentiated adenocarcinomas overlapping with renal medullary carcinoma. Hum Pathol. 2017;67:134–45.
12. Sandberg JK, Mullen EA, Cajaiba MM, Smith EA, Servaes S, Perlman EJ, et al. Imaging of renal medullary carcinoma in children and young adults: a report from the Children's Oncology Group. Pediatr Radiol. 2017;47(12):1615–21.
13. Blitman NM, Berkenblit RG, Rozenblit AM, Levin TL. Renal Medullary Carcinoma: CT and MRI Features. Am J Roentgenol 2005;185(1):268–72.
14. •• Chung EM, Lattin GE, Fagen KE, Kim AM, Pavio MA, Fehringer AJ, et al. Renal tumors of childhood: radiologic-pathologic correlation part 2. The 2nd Decade: From the Radiologic Pathology Archives. RadioGraphics. 2017;37(5):1538–58. **This article presents the radiological and pathological correlation of different renal masses. Furthermore, describes distinguishing clinical and imaging features in order to make appropiate differential diagnoses.**

15. Li T, Chen J, Jiang Y, Ning X, Peng S, Wang J, et al. Multilocular cystic renal cell neoplasm of low malignant potential: a series of 76 cases. Clin Genitourin Cancer. 2016;14(6):e553–7.
16. Tretiakova M, Mehta V, Kocherginsky M, Minor A, Shen SS, Sirintrapun SJ, et al. Predominantly cystic clear cell renal cell carcinoma and multilocular cystic renal neoplasm of low malignant potential form a low-grade spectrum. Virchows Arch. 2018;473(1):85–93.
17. Bhatt JR, Jewett MAS, Richard PO, Kawaguchi S, Timilshina N, Evans A, et al. Multilocular cystic renal cell carcinoma: pathological T staging makes no difference to favorable outcomes and should be reclassified. J Urol. 2016;196(5):1350–5.
18. Williamson SR, Cheng L. Clear cell renal cell tumors: not all that is "clear" is cancer. Urol Oncol. 2016;34(7):292.e17–22.
19. Gürel S, Narra V, Elsayes KM, Siegel CL, Chen ZE, Brown JJ. Subtypes of renal cell carcinoma: MRI and pathological features. Diagn Interv Radiol. 2013;19(4):304–11.
20. Ghosh P, Kaushik S. Multilocular cystic renal cell carcinoma: a rare, unique entity and diagnostic challenge. Arch Iran Med. 2014;17(2):129–32.
21. Adsay NV, Eble JN, Srigley JR, Jones EC, Grignon DJ. Mixed epithelial and stromal tumor of the kidney. Am J Surg Pathol. 2000;24(7):958–70.
22. Zhao M, He X, Teng X. Mucinous tubular and spindle cell renal cell carcinoma: a review of clinicopathologic aspects. Diagn Pathol. 2015;10(1):168.
23. Kenney PA, Vikram R, Prasad SR, Tamboli P, Matin SF, Wood CG, et al. Mucinous tubular and spindle cell carcinoma (MTSCC) of the kidney: a detailed study of radiological, pathological and clinical outcomes. BJU Int. 2015;116(1):85–92.
24. Cornelis F, Ambrosetti D, Rocher L, Derchi LE, Renard B, Puech P, et al. CT and MR imaging features of mucinous tubular and spindle cell carcinoma of the kidneys. A multi-institutional review. Eur Radiol. 2017;27(3):1087–95.
25. Sahni VA, Hirsch MS, Sadow CA, Silverman SG. Mucinous tubular and spindle cell carcinoma of the kidney: imaging features. Cancer Imaging. 2012;12(1):66–71.
26.•• Kay FU, Pedrosa I. Imaging of solid renal masses. Radiol Clin N Am. 2017;55(2):243–58. **This article emphazise the actual role of imaging and its different modalities in order to characterise benign and malignant renal lesions.**
27. Wobker SE, Williamson SR. Modern pathologic diagnosis of renal oncocytoma. J Kidney Cancer VHL. 2017;4(4):1–12.
28.• Lopes Vendrami C, Parada Villavicencio C, DeJulio TJ, Chatterjee A, Casalino DD, Horowitz JM, et al. Differentiation of solid renal tumors with multiparametric MR imaging. RadioGraphics. 2017;37(7):2026–42. **This article describe the imaging and pathologic characteristics of the most common renal tumors. As well as the MRI imaging diagnostic approach of these renal masses.**
29. Lou L, Teng J, Lin X, Zhang H. Ultrasonographic features of renal oncocytoma with histopathologic correlation. J Clin Ultrasound. 2014;42(3):129–33.
30. Young JR, Coy H, Kim HJ, Douek M, Lo P, Pantuck AJ, et al. Performance of relative enhancement on multiphasic MRI for the differentiation of clear cell renal cell carcinoma (RCC) from papillary and chromophobe RCC subtypes and oncocytoma. Am J Roentgenol. 2017;208(4):812–9.
31. Kao SL, Hsu YH, Kuo HC. Renal oncocytoma with specific imaging findings. Tzu Chi Med J. 2010;22(1):36–8.
32. Wu J, Zhu Q, Zhu W, Zhang H. Metanephric adenoma with diffuse calcifications: a case report. Oncol Lett. 2015;10(3):1816–8.
33. Zhu Q, Zhu W, Wu J, Chen W, Wang S. The clinical and CT imaging features of metanephric adenoma. Acta Radiol. 2014;55(2):231–8.
34. Mantoan Padilha M, Billis A, Allende D, Zhou M, Magi-Galluzzi C. Metanephric adenoma and solid variant of papillary renal cell carcinoma: common and distinctive features. Histopathology. 2013;62(6):941–53.
35. Küpeli S, Baydar DE, Çanakl F, Yalçn B, Kösemehmetoğlu K, Tekgül S, et al. Metanephric adenoma in a 6-year-old child with hemihypertrophy. J Pediatr Hematol Oncol. 2009;31(6):453–5.
36. Eble JN. Angiomyolipoma of kidney. Semin Diagn Pathol. 1998;15(1):21–40.
37. Nelson CP, Sanda MG. Contemporary diagnosis and management of renal angiomyolipoma. J Urol. 2002;168(4 Pt 1):1315–25.
38. Tsui WM, Colombari R, Portmann BC, Bonetti F, Thung SN, Ferrell LD, et al. Hepatic angiomyolipoma: a clinicopathologic study of 30 cases and delineation of unusual morphologic variants. Am J Surg Pathol. 1999;23(1):34–48.
39. Lane BR, Aydin H, Danforth TL, Zhou M, Remer EM, Novick AC, et al. Clinical correlates of renal angiomyolipoma subtypes in 209 patients: classic, fat poor, tuberous sclerosis associated and epithelioid. J Urol. 2008;180(3):836–43.
40. Zhu J, Li H, Ding L, Cheng H, Zhu J, Li H, et al. Imaging appearance of renal epithelioid angiomyolipoma: a case report and literature review. Medicine (Baltimore). 2018;97(1):1–4.
41. Raman SP, Hruban RH, Fishman EK. Beyond renal cell carcinoma: rare and unusual renal masses. Abdom Imaging. 2012;37(5):873–84.
42. Liu Y, Qu F, Cheng R, Ye Z. CT-imaging features of renal epithelioid angiomyolipoma. World J Surg Oncol. 2015;13(1):9–14.
43. Park JH, Lee C, Suh JH, Kim G, Song B, Moon KC. Renal epithelioid angiomyolipoma: histopathologic review, immunohistochemical evaluation and prognostic significance. Pathol Int. 2016;66(10):571–7.
44. Tsukada J, Jinzaki M, Yao M, Nagashima Y, Mikami S, Yashiro H, et al. Epithelioid angiomyolipoma of the kidney: radiological imaging. Int J Urol. 2013;20(11):1105–11.
45. Ryan MJ, Francis IR, Cohan RH, Davenport MS, Weizer A, Hafez K, et al. Imaging appearance of renal epithelioid angiomyolipomas. J Comput Assist Tomogr. 2013;37(6):957–61.
46. Qiu T, Ling W, Lu Q, Lu C, Luo Y. Contrast-enhanced ultrasound in diagnosis of epithelioid renal angiomyolipoma with renal vein and inferior vena cava extension. J Med Ultrason. 2016;43(3):427–30.
47. Zhong Y, Shen Y, Pan J, Wang Y, An Y, Guo A, et al. Renal epithelioid angiomyolipoma: MRI findings. Radiol Med. 2017;122(11):814–21.
48. Chuang CK, Lin HCA, Tasi HY, Lee KH, Kao Y, Chuang FL, et al. Clinical presentations and molecular studies of invasive renal epithelioid angiomyolipoma. Int Urol Nephrol. 2017;49(9):1527–36.
49. Zeng X, Huang H, Li J, Peng J, Zhang J. The clinical and radiological characteristics of inflammatory myofibroblastic tumor occurring at unusual sites. Biomed Res Int. 2018;2018:1–8.
50. Babu P, Kalpana Kumari MK, Nagaraj HK, Mysorekar VV. Inflammatory pseudotumor of kidney masquerading as renal carcinoma. J Cancer Res Ther. 2015;11(3):668.
51. Patnana M, Sevrukov AB, Elsayes KM, Viswanathan C, Lubner M, Menias CO. Inflammatory pseudotumor: the great mimicker. Am J Roentgenol. 2012;198(3):12–5.
52. Lee NG, Alexander MP, Xu H, Wang DS. Renal inflammatory myofibroblastic tumor: a case report and comprehensive review of literature. World J Oncol. 2011;2(2):85–8.
53. Dogan MS, Doganay S, Koc G, Gorkem SB, Unal E, Ozturk F, et al. Inflammatory myofibroblastic tumor of the kidney and bilateral lung nodules in a child mimicking Wilms tumor with lung metastases. J Pediatr Hematol Oncol. 2015;37(6):390–3.
54. Zhu L, Li J, Liu C, Ding W, Lin F, Guo C, et al. Pulmonary inflammatory myofibroblastic tumor versus IgG4-related inflammatory pseudotumor: differential diagnosis based on a case series. J Thorac Dis. 2017;9(3):598–609.

55. Kramer S, Meadows AT, Jarrett P, Evans AE. Incidence of childhood cancer: experience of a decade in a population-based registry. J Natl Cancer Inst. 1983;70(1):49–55.
56. Hollowood K, Fletcher CD. Rhabdomyosarcoma in adults. Semin Diagn Pathol. 1994;11(1):47–57.
57. Furlong MA, Mentzel T, Fanburg-Smith JC. Pleomorphic rhabdomyosarcoma in adults: a clinicopathologic study of 38 cases with emphasis on morphologic variants and recent skeletal muscle-specific markers. Mod Pathol. 2001;14(6):595–603.
58. Grignon DJ, McIsaac GP, Armstrong RF, Wyatt JK. Primary rhabdomyosarcoma of the kidney: a light microscopic, immunohistochemical, and electron microscopic study. Cancer. 1988;62(9):2027–32.
59. Alaa S, Haneen A-M. Rhabdomyosarcoma of the kidney. J Pediatr Surg Case Rep. 2018;32:62–7.
60. Seifert RP, McNab P, Sexton WJ, Sawczyn KK, Smith P, Coppola D, et al. Rhabdomyomatous differentiation in Wilms tumor pulmonary metastases: a case report and literature review. Ann Clin Lab Sci. 2012;42(4):409–16.
61. Hakky TS, Gonzalvo AA, Lockhart JL, Rodriguez AR. Primary Ewing sarcoma of the kidney: a symptomatic presentation and review of the literature. Ther Adv Urol. 2013;5(3):153–9.
62. Iwamoto Y. Diagnosis and treatment of Ewing's sarcoma. Jpn J Clin Oncol. 2007;37(2):79–89.
63. Pakravan A, Vo T-M, Sandomirsky M, Bastani B. Kidney diseases primary Ewing sarcoma of kidney in an elderly. Iran J Kidney Dis. 2012;6:307–10.
64. Thyavihally YB, Tongaonkar HB, Gupta S, Kurkure PA, Amare P, Muckaden MA, et al. Primitive neuroectodermal tumor of the kidney: a single institute series of 16 patients. Urology. 2008;71(2):292–6.
65. Angel JR, Alfred A, Sakhuja A, Sells RE, Zechlinski JJ. Ewing's sarcoma of the kidney. Int J Clin Oncol. 2010;15(3):314–8.
66. Cuesta Alcalá JA, Solchaga Martínez A, Caballero Martínez MC, Gómez Dorronsoro M, Pascual Piédrola I, Ripa Saldías L, et al. Primary neuroectodermal tumor (PNET) of the kidney: 26 cases. Current status of its diagnosis and treatment. Arch Esp Urol. 2001;54(10):1081–93.
67. Michal M, Syrucek M. Benign mixed epithelial and stromal tumor of the kidney. Pathol Res Pract. 1998;194(6):445–8.
68. Podduturi V, Guileyardo JM. Mixed epithelial and stromal tumors of the kidney discovered incidentally at autopsy. Proc (Bayl Univ Med Cent). 2015;28(2):224–6.
69. Chu LC, Hruban RH, Horton KM, Fishman EK. Mixed epithelial and stromal tumor of the kidney: radiologic-pathologic correlation. Radiographics. 2010;30(6):1541–51.
70. Gallo GE, Penchansky L. Cystic nephroma. Cancer. 1977;39(3):1322–7.
71. Granja MF, O'Brien AT, Trujillo S, Mancera J, Aguirre DA. Multilocular cystic nephroma: a systematic literature review of the radiologic and clinical findings. Am J Roentgenol. 2015;205(6):1188–93.
72. Madewell JE, Goldman SM, Davis CJ, Hartman DS, Feigin DS, Lichtenstein JE. Multilocular cystic nephroma: a radiographic-pathologic correlation of 58 patients. Radiology. 1983;146(2):309–21.
73. Charu A, Arvind A, Palak A, Minakshi B. Multilocular cystic nephroma: a rare presentation in a young female. J Clin Exp Pathol. 2017;07(04):1–2.
74. Kalapurakal JA, Dome JS, Perlman EJ, Malogolowkin M, Haase GM, Grundy P, et al. Management of Wilms' tumour: current practice and future goals. Lancet Oncol. 2004;5(1):37–46.
75. Huff V. Wilms' tumours: about tumour suppressor genes, an oncogene and a chameleon gene. Nat Rev Cancer. 2011;11(2):111–21.
76. Scott RH, Stiller CA, Walker L, Rahman N. Syndromes and constitutional chromosomal abnormalities associated with Wilms tumour. J Med Genet. 2006;43(9):705–15.
77. Kalish JM, Doros L, Helman LJ, Hennekam RC, Kuiper RP, Maas SM, et al. Surveillance recommendations for children with overgrowth syndromes and predisposition to Wilms tumors and hepatoblastoma. Clin Cancer Res. 2017;23(13):e115–22.
78. Zuppan CW, Beckwith JB, Luckey DW. Anaplasia in unilateral Wilms' tumor: a report from the National Wilms' Tumor Study pathology center. Hum Pathol. 1988;19(10):1199–209.
79. Lowe LH, Isuani BH, Heller RM, Stein SM, Johnson JE, Navarro OM, et al. Pediatric renal masses: Wilms tumor and beyond. Radiographics. 2000;20(6):1585–603.
80. D'Angio GJ, Breslow N, Beckwith JB, Evans A, Baum H, de Lorimier A, et al. Treatment of Wilms' tumor. Results of the third National Wilms' Tumor Study. Cancer. 1989;64(2):349–60.
81. Huszno J, Starzyczny-Słota D, Jaworska M, Nowara E. Adult Wilms' tumor—diagnosis and current therapy. Cent European J Urol. 2013;66(1):39–44.
82. Metzger ML, Dome JS. Current therapy for Wilms' tumor. Oncologist. 2005;10(10):815–26.
83. Gow KW, Barnhart DC, Hamilton TE, Kandel JJ, Chen MKS, Ferrer FA, et al. Primary nephrectomy and intraoperative tumor spill: report from the Children's oncology group (COG) renal tumors committee. J Pediatr Surg. 2013;48(1):34–8.
84. Idrissi-Serhrouchni K, El-Fatemi H, El Madi A, Benhayoun K, Chbani L, Harmouch T, et al. Primary renal teratoma: a rare entity. Diagn Pathol. 2013;8:107.
85. Nirmal TJ, Krishnamoorthy S, Korula A. Primary intrarenal teratoma in an adult: a case report and review of literature. Indian J Urol. 2009;25(3):404–6.
86. Yoo J, Park S, Jung Lee H, Jin Kang S, Kee KB. Primary carcinoid tumor arising in a mature teratoma of the kidney: a case report and review of the literature. Arch Pathol Lab Med. 2002;126(8):979–81.
87. Otani M, Tsujimoto S, Miura M, Nagashima Y. Intrarenal mature cystic teratoma associated with renal dysplasia: case report and literature review. Pathol Int. 2001;51(7):560–4.
88. Urban BA, Fishman EK. Renal lymphoma: CT patterns with emphasis on helical CT. Radiographics. 2000;20(1):197–212.
89. Sheth S, Ali S, Fishman E. Imaging of renal lymphoma: patterns of disease with pathologic correlation. Radiographics. 2006;26(4):1151–68.
90. Purysko AS, Westphalen AC, Remer EM, Coppa CP, Leão Filho HM, Herts BR. Imaging manifestations of hematologic diseases with renal and perinephric involvement. Radiographics. 2016;36(4):1038–54.
91. Chen X, Hu D, Fang L, Chen Y, Che X, Tao J, et al. Primary renal lymphoma: a case report and literature review. Oncol Lett. 2016;12(5):4001–8.
92. Donow C, Pipeleers-Marichal M, Schröder S, Stamm B, Heitz PU, Klöppel G. Surgical pathology of gastrinoma. Site, size, multicentricity, association with multiple endocrine neoplasia type 1, and malignancy. Cancer. 1991;68(6):1329–34.
93. Katkoori D, Samavedi S, Jorda M, Block NL, Manoharan M. A rare case of renal gastrinoma. ScientificWorldJournal. 2009;9:501–4.
94. Howard TJ, Sawicki M, Lewin KJ, Steel B, Bhagavan BS, Cummings OW, et al. Pancreatic polypeptide immunoreactivity in sporadic gastrinoma: relationship to intraabdominal location. Pancreas. 1995;11(4):350–6.
95. Dyer R, DiSantis DJ, McClennan BL. Simplified imaging approach for evaluation of the solid renal mass in adults. Radiology. 2008;247(2):331–43.
96. Herrera-Caceres JO, Finelli A, Jewett MAS. Renal tumor biopsy: indicators, technique, safety, accuracy results, and impact on treatment decision management. World J Urol. 2018;0123456789.

97. Reinhard R, Van der Zon-Conijn M, Smithuis R. Kidney Solid Masses. In: Radiology Assistant. June, 2016. http://www.radiologyassistant.nl/en/p571eea20ec282/kidney-solid-masses.html. Accessed 12 May 2019.
98. Bagheri MH, Ahlman MA, Lindenberg L, Turkbey B, Lin J, Cahid Civelek A, et al. Advances in medical imaging for the diagnosis and management of common genitourinary cancers. Urol Oncol. 2017;35(7):473–91.
99. Volpe A, Finelli A, Gill IS, Jewett MAS, Martignoni G, Polascik TJ, et al. Rationale for percutaneous biopsy and histologic characterisation of renal tumours. Eur Urol. 2012;62(3):491–504.
100. Baughman RP, Teirstein AS, Judson MA, Rossman MD, Yeager H, Bresnitz EA, et al. Clinical characteristics of patients in a case control study of sarcoidosis. Am J Respir Crit Care Med. 2001;164(10):1885–9.
101. Roudenko A, Murillo P, Akers S, Koo CW. Renal sarcoid: pseudotumoral radiologic manifestations and pathologic correlation. Radiol Case Rep. 2012;7(2):599.
102. Koyama T, Ueda H, Togashi K, Umeoka S, Kataoka M, Nagai S. Radiologic manifestations of sarcoidosis in various organs. Radiographics. 2004;24(1):87–104.